A Statistical Thermodynamic Model for Cross-Bridge Mediated Condensation of Vesicles†

Itzhak Farbman-Yogev, Yardena Bohbot-Raviv, and Avinoam Ben-Shaul*

Department of Physical Chemistry and the Fritz Haber Research Center, The Hebrew University, Jerusalem 91904, Israel

Received: May 20, 1998; In Final Form: July 10, 1998

The phase behavior of a solution containing a mixture of large and small, cross-bridging ("two-sided sticker") particles is studied using a lattice model analyzed with the aid of mean-field calculations and Monte Carlo simulations. Neither the large nor the small particles interact with each other (except for excluded volume effects). However, the small particles can adsorb onto the surface of one or two large particles, in the latter case providing a cross-bridge, i.e., an adhesive bond, between the large particles. The formulation of the model is motivated by experimental studies involving aqueous solutions of vesicles (the large particles) and biotin−avidin−biotin cross-bridges. This system exhibits a first-order phase transition from a dilute to a condensed phase of vesicles once the average number of stickers per vesicle exceeds a certain threshold value. The statistical thermodynamic description of the system becomes particularly simple upon (Legendre) transformation from the two-component canonical ensemble to a "mixed" ensemble involving a constant chemical potential of the cross-bridge particles. The phase separation behavior of the system is calculated for two sets of molecular parametrs, revealing good qualitative agreement with relevant experiments.

I. Introduction

In this paper we present a simple statistical thermodynamic model to describe a rather special condensation phenomenon: the aggregation of large particles mediated by small, cross-bridge particles. These cross-bridges induce a "specific adhesion" process, which, above a certain critical concentration, can lead to a macroscopic phase separation involving dilute and concentrated phases of the large particles.

The large particles in the model system that we have in mind are lipid vesicles, i.e., closed, spheroidal but slightly deformable, lipid bilayers, of diameters in the range of 50−100 nm, embedded in an aqueous solution. A common example of a cross-bridge particle is a biotin−avidin−biotin complex. The avidin receptor has four biotin binding sites, two on each side.[1] If some of the lipids constituting the vesicle membrane are biotinated (i.e., chemically connected to biotin residues through their hydrophilic headgroups), then by binding one or two biotin ligands on *both* of its sides, the water-soluble avidin can form a cross-bridge between two vesicles. This biotin−avidin−biotin bridge is often used as a model system for studying *specific adhesion* phenomena, which are of great interest in a variety of biological systems.[1−3]

A number of experimental and theoretical studies have focused on studying the kinetic pathways and metastable structures characterizing the avidin-mediated aggregation of biotinated vesicles and related systems.[4−6] Many other studies have concentrated on measuring and interpreting the forces and energies involved in avidin−biotin binding and cross-bridging, and their dependence on factors such as membrane fluidity and elasticity.[7−16] Among the conclusions of these studies is that the noncovalent avidin−biotin bond is generally much stronger than the "hydrophobic" bond between the hydrocarbon tail of the biotinated lipid and the vesicle membrane. Thus, once the avidin is bound to a biotinated membrane lipid, pulling it off the vesicle would result in detachment of the hydrophobic tail from the membrane rather than in dissociation of the avidin−biotin bond.[8−13]

The size and shape of the aggregates formed upon adding avidin to a solution containing biotinated vesicles may strongly depend on *kinetic* factors associated with the efficient and essentially irreversible binding of the avidin to the biotinated lipids. The rapid, avidin-mediated adhesion of vesicles can result in the formation of long-lived (e.g, fractal) aggregates.[4−6] However, the long-time behavior of this system may be quite different since cross-bridged vesicles can still dissociate by breaking the weaker bonds between the biotinated lipids and the vesicle membrane. In other words, the equilibrium state of the system is most likely goverened by the formation and dissociation of these biotinated lipid−vesicle bonds and not the avidin−biotin bonds. Indeed, recent experiments[17] reveal that in a solution containing a small concentration of receptors, say five streptavidin molecules (A) per vesicle (V) (each vesicle containing, on average, 80 biotinated lipids), the vesicles initially aggregate into large clusters. However, after a while these clusters redisperse into isolated vesicles. Furthermore, the experiments show that the long-time behavior of these solutions is independent of the mode of preparing the dispersion. Namely, the state of aggregation depends only on the avidin to biotin (A/V) ratio, indicating that the system has reached true thermodynamic equilibrium. One clear conclusion from these experiments is that macroscopic phase separation takes place once $A/V \equiv \sigma$ exceeds a certain critical value ($\sigma \approx 10$, for vesicles containing 80 biotinated headgroups).

Our goal in this paper is to explain, qualitatively, the equilibrium phase behavior of a solution containing biotinated vesicles and avidin cross-bridges. More generally, we are interested in the phase behavior of a system containing large particles, between which attraction takes place upon adding small, cross-bridging particles into the mixture. To this end

† This paper is dedicated to Raphy Levine, our colleague, mentor, and friend, on the occasion of his 60th birthday.

10.1021/jp9823300 CCC: $15.00
Published on Web 09/17/1998

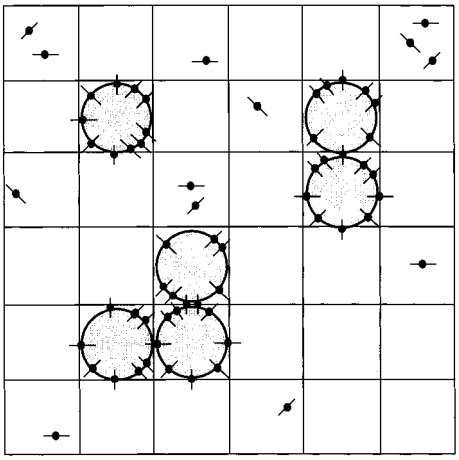

Figure 1. Schematic illustration of the model on a 2D square lattice. Each lattice site can accommodate one vesicle (large particle). The cross-bridging "stickers" are either free (f), i.e., dispersed among the vacant sites, or adsorbed (a) onto an exposed surface of a vesicle, or adsorbed onto the surfaces of two neighboring vesicles, thus forming an adhesive bond (b).

we have formulated a simple lattice model, each cell of which can contain one vesicle—thus accounting for vesicle−vesicle excluded volume interactions. We ignore the nonspecific long-range attractions between vesicles but explicitly include the indirect attractions mediated by the avidin cross-bridges. Following the experiments reported in ref 17, we assume that the number of biotinated lipids greatly exceeds the number of avidin receptors. For these conditions it is safe to assume that all the biotin binding sites on the avidin receptor are occupied and hence all cross-linkers (hereafter also referred to as "stickers") are actually $(BL)_2$−A-$(BL)_2$ complexes, with BL denoting a biotinated lipid molecule. On the basis of the notion that the BL-vesicle bond is considerably weaker than the BL−A bond, the phase behavior of the system can be derived by treating it as a mixture of vesicles and $(BL)_2$−A−$(BL)_2$ stickers.

II. Theory

A. Model. Consider an aqueous solution of total volume V and temperature T, containing two kinds of particles: N large particles representing the vesicles and n small particles representing the "stickers". We assume that the vesicles are slightly deformable spheres, all of the same diameter d. The stickers, corresponding to the tight complex formed between streptavidin and four biotinated lipids (two on each side), may be viewed as a peg; each of its ends can adsorb onto the surface of one vesicle. Two vesicles form a bound pair when they are bridged by one or several stickers, as illustrated in Figure 1. This *sticker-induced adhesion* between vesicles can lead to their aggregation and eventaully to a macroscopic phase transition from a dilute to a condensed phase of vesicles.

The phase behavior of this system will be analyzed on the basis of a lattice model, which will be solved using a mean-field approximation. The use of the lattice ensures that excluded volume interactions between the vesicles are taken into account. More significantly, the model explictly accounts for sticker−vesicle adsorption and sticker-mediated attraction between the vesicles. Sticker−sticker and sticker−vesicle excluded volume interactions are taken into account in an approximate fashion. Some of the qualitative conclusions derived from the mean-field analysis will be tested against Monte Carlo (MC) simulations of a 2D model system.

Recall that in the mean-field approximation neither the dimensionality nor the exact geometry of the lattice is taken into account; the only relevant structural parameter is the lattice coordination number, z. Nevertheless, for concreteness, let us regard the system as a 3D cubic lattice, consisting of M sites of volume $v = V/M = d^3$, so that each site can contain exactly one vesicle, Figure 1. Since the stickers are much smaller than the vesicles, each vacant lattice site can contain a large number of stickers, s; s is approximately equal to the ratio between the vesicle's volume and the volume of a biotin−avidin−biotin cross-bridge.

Three kinds of stickers are possible in the system: (i) "bridge" (b) stickers connecting two nearest-neighbor vesicles; (ii) "adsorbed" (a) stickers whose one end is anchored to the surface of a vesicle and the other is free; (iii) "free" (f) stickers both ends of which are free. We shall use ν_b to denote the maximal number of stickers that can serve as connectors between the same two, nearest-neighbor vesicles. In principle, ν_b depends on the contact area between adjacent vesicles, which, in turn, depends on their deformability. The maximal number of stickers that can adsorb onto the surface of one vesicle will be denoted as $z\nu_a$. In our lattice model this implies that ν_a is the maximal number of stickers that can populate a face of the lattice separating between two neighboring sites, one empty and the other occupied by a vesicle. Finally, we use $z\nu_f/2 = s$ to denote the maximal number of free stickers per vacant lattice site. (We may regard ν_f as the maximal number of stickers on a lattice face separating two vacant sites.) From this description it follows that we can imagine the a and b stickers as moving on the faces of the lattice cells, whereas the f stickers populate the vacant lattice cells. The conditions of experimental relevance correspond to $\nu_f \gg \nu_a > \nu_b$.

The energy change involved in the adsorption of one end of a sticker to a vesicle will be denoted as $-kT\epsilon_a$, where k is Boltzmann's constant and T the absolute temperature; i.e., $\epsilon_a > 0$ is the sticker−vesicle interaction energy, in units of kT. We ignore nonadditivity effects, assuming that the adsorption energy is independent of the number of adsorbed stickers. Similarly, we assume that the binding energy associated with the formation of a sticker bridge between two vesicles, $kT\epsilon_b$, is independent of the number of bridges. Typically, $\epsilon_b \approx 2\epsilon_a$; yet, we shall treat ϵ_b and ϵ_a as independent variables. Note that these energies are measured with respect to the energy of the free sticker, $\epsilon_f \equiv 0$.

B. Free Energy. Every configuration, $\{C\}$, of the N vesicles on the M lattice sites dictates the number of α sites, m_α, available to the three types of stickers in the system; α = f, a, b. Since free stickers can only be found in vacant lattice cells, $m_f = s(M - N) = (1/2)z\upsilon_f M(1 - \rho)$, where $\rho = N/M$ is the density (volume fraction) of vesicles in the system. In principle, one can include in m_f the small fraction of free stickers that may be present in the "corners" of a site already occupied by a vesicle. This refinement does not affect our conclusions and will therefore be ignored.

Bridge stickers, connecting nearest-neighbor vesicles, are necessarily confined to the faces between pairs of lattice sites occupied by vesicles. Using the above defintion of ν_b we have $m_b = \nu_b N_{vv}$ where N_{vv} is the number of doubly occupied pairs of nearest-neighbor sites. For m_a we have $m_a = \nu_a N_{0v} + (2\nu_a - \nu_b)N_{vv}$, where N_{0v} is the number of singly occupied site pairs. The second term in m_a accounts for those adsorbed stickers at doubly occupied faces that do not form bridges.

Consider now a particular configuration, $\{C\}$, of the N vesicles on the M lattice sites. The Helmholtz free energy *of*

the stickers corresponding to this "*frozen*" configuration, $F_s(\{C\})$, is given by

$$F_s = \sum_\alpha [n_\alpha \epsilon_\alpha + m_\alpha S_\alpha] \tag{1}$$

where S_α is the entropy, per sticker site, corresponding to stickers of type α. Note that in (1) and elsewhere in this paper we measure energies, free energies, and chemical potentials in units of kT and entropies in units of k.

Assuming that except for excluded volume (or area) effects the stickers do not interact with each other, we can write

$$-S_\alpha = \theta_\alpha \ln \theta_\alpha + (1 - \theta_\alpha) \ln(1 - \theta_\alpha) \tag{2}$$

where $\theta_\alpha = n_\alpha/m_\alpha$ is the fractional occupation of α sites by stickers and n_α is the number of stickers of type α; $\sum_{(\alpha)} n_\alpha = n$. Note that θ_f is, in fact, a volume fraction whereas θ_a and θ_b are area fractions.

The equilibrium values of the n_α's, and hence the θ_α's, can be determined by minimzing F_s with respect to these variables. The minimum conditions lead, as expected, to the equality of chemical potentials

$$\mu_f = \mu_a = \mu_b \equiv \mu_s \equiv \ln \lambda \tag{3}$$

with

$$\mu_\alpha = \ln \frac{\theta_\alpha}{1 - \theta_\alpha} - \epsilon_\alpha \tag{4}$$

denoting the chemical potential of α-type stickers; $\lambda = \exp(\mu_s)$ is the absolute activity of the stickers. Since $\epsilon_f = 0$, we find $\lambda = \theta_f/(1 - \theta_f)$. Also, since typically $\epsilon_b \approx 2\epsilon_a > 10$, it follows that $\theta_b \gg \theta_a \gg \theta_f$ and hence $\theta_f \ll 1$, implying $\lambda \simeq \theta_f$; i.e., the activity is equal to the concentration of free stickers.

At this point we introduce the mean-field approximation, replacing N_{vv} and N_{0v} by their values corresponding to a random distribution of the vesicles; namely $N_{vv} = (1/2)zM\rho^2$ and $N_{0v} = zM\rho(1 - \rho)$. This yields

$$m_f = \frac{1}{2} zM(1 - \rho)\nu_f \tag{5}$$

$$m_a = zM_\rho(1 - \rho)\nu_a + \frac{1}{2} zM\rho^2(2\nu_a - \nu_b) = \frac{1}{2} zM\rho(2\nu_a - \rho\nu_b)$$

$$m_b = \frac{1}{2} zM\rho^2 \nu_b$$

Using these m_α's in (1) we obtain the mean-field value of the stickers free energy, $\bar{F}_s$. Adding the entropy S_v associated with the (random) distribution of the N vesicles over the M lattice sites, we obtain the total free energy of the system

$$F = \bar{F}_s + M[\rho \ln \rho + (1 - \rho) \ln(1 - \rho)] \tag{6}$$

where the expression in square brackets is the vesicles' entropy per lattice site, $-S_v/M$.

To analyze the phase behavior of the system, it is convenient to perform a Legendre transformation from the Helmholtz free energy $F = F(N, n, M, T)$ to the "mixed" thermodynamic potential $\Gamma = \Gamma(N, \mu_s, M, T)$,

$$\Gamma = F - n\mu_s \tag{7}$$

$$= -MS_v + \sum_\alpha m_\alpha \ln(1 - \theta_\alpha) \tag{8}$$

$$= -MS_v - \sum_\alpha m_\alpha \ln(1 + \lambda\xi_\alpha)$$

where in the last equality we have used the relation $\theta_\alpha = \lambda\xi_\alpha/(1 + \lambda\xi_\alpha)$ with $\xi_\alpha \equiv \exp(\epsilon_\alpha)$.

The above expression for Γ can now be used to evaluate the (dimensionless) osmotic pressure in the system, $P = -(\partial F/\partial M)_{T,N,n} = -(\partial\Gamma/\partial M)_{T,N,\lambda}$, as well as the chemical potential of the vesicles, $\mu_v = (\partial F/\partial N)_{T,M,n} = (\partial\Gamma/\partial N)_{T,M,\lambda}$. These relations yield

$$P = -\ln(1 - \rho) - \frac{1}{2}\chi\rho^2 + \frac{1}{2} z\nu_f \ln(1 + \lambda) \tag{9}$$

$$\mu_v = \ln\left(\frac{\rho}{1 - \rho}\right) - \chi\rho - z\nu_a \ln(1 + \lambda\xi_a) + \frac{1}{2} z\nu_f \ln(1 + \lambda) \tag{10}$$

with χ given by

$$\chi = z\nu_b \ln\left(\frac{1 - \theta_a}{1 - \theta_b}\right) = z\nu_b \ln\left(\frac{1 + \lambda\xi_b}{1 + \lambda\xi_a}\right) \tag{11}$$

The first two terms in the equation of state, (9), constitute the familiar expression for the pressure of an interacting lattice gas of density ρ in the Bragg−Williams approximation.[18] In the case of an ordinary lattice gas the interaction parameter χ is simply related to ω, the pair potential between two particles occupying nearest-neighbor sites; $\chi = z\omega/kT$. In our system this direct interaction potential is replaced by the sticker-mediated interaction defined by (11), which depends on the stickers' chemical potential, $\mu_s = \ln \lambda$, and the adsorption and binding energies ξ_a, ξ_b. Indeed, it is not difficult to show that $kT\chi/z \equiv \omega_{eff}$ is the (negative) free energy change associated with bringing two remote vesicles into contact (nearest-neighbor positions), at constant chemical potential of the stickers.

The last term in (9) is the contribution to the pressure arising from the free stickers in the system. Recall that $z\nu_f/2$ is the number of stickers per lattice site. Note also that the adsorbed and bound stickers do not contribute to the pressure in the system. (Of course, the bound stickers affect, through χ, the number of vesicle clusters and hence the pressure in the system.) In analogy to (9) the first two terms in (10) correspond to the chemical potential of an interacting lattice gas of vesicles of density ρ. The two last terms in (10) represent the change in the free energy of the system (the reversible work), associated with adding a single ("immobile") vesicle to a system already containing stickers with the given chemical potential μ_s.

C. Phase Behavior. Under certain conditions the sticker-mediated interactions between the vesicles can induce a macroscopic phase separation, with the two coexisting phases, hereby denoted as d ("dilute") and c ("condensed"), characterized by different vesicle densities and different sticker concentrations. At a given temperature, there are three equilibrium conditions: equality of pressures $P^{(d)}=P^{(c)}$, vesicle chemical potentials $\mu^{(d)}{}_v = \mu^{(c)}{}_v$, and stickers' chemical potentials $\mu_s^{(d)} = \mu_s^{(c)}$. The third condition is automatically ensured if the pressures and chemical potentials of the coexisting phases are calculated using (9) and (10) for the same value of λ in the two phases. In other words, our coexistence equations are

$$P^{(d)}(\rho^{(d)}; \lambda, T) = P^{(c)}(\rho^{(c)}; \lambda, T) \quad (12)$$

$$\mu_v^{(d)}(\rho^{(d)}; \lambda, T) = \mu_v^{(c)}(\rho^{(c)}; \lambda, T) \quad (13)$$

Using (9) and (10) in (11) and (12), we obtain the equation describing the coexistence curve, which separates between the one-phase and two-phase regimes

$$\chi_{\text{coexistence}} = \frac{2}{|1 - 2\rho|} \ln\left(\frac{1 + |1 - 2\rho|}{1 - |1 - 2\rho|}\right) \quad (14)$$

The spinodal curve, corresponding to $\partial^2 P/\partial\rho^2 = 0$, is given by

$$\chi_{\text{spinodal}} = \frac{1}{\rho(1 - \rho)} \quad (15)$$

Both of the above equations imply the existence of a critical point at $\rho = \rho_c = 0.5$ and $\chi = \chi_c = 4$. Not surprisingly, the shape of the coexistence and spinodal curves, as well as the critical values of χ and ρ, are those of an ordinary lattice gas.[18] The only diffrence between our system and the lattice gas is that in our case the magnitude of the interaction parameter, χ, is controlled by the stickers' chemical potential through (11). Substituting (11) into (14) and (15), we obtain the coexistence and spinodal curves in the $\rho-\lambda$ plane. These curves depend of course on the molecular parameters z, ν_b, ϵ_a, ϵ_b. In Figure 2 we show these curves for $z = 12$, $\nu_b = 4$, and $\epsilon_b = 2\epsilon_a = 10$. In the $\rho-\lambda$ plane the dilute and concentrated phases, at coexistence, are connected by horizontal tie-lines. Experimentally, the overall sticker concentration n/M or, equivalently, the sticker-to-vesicle concentration ratio $\sigma \equiv n/N$, are more convenient control parameters than λ. Thus, our numerical results in the next section will be reported in terms of $\sigma-\rho$ diagrams. In this representation the coexistence curves are not symmetrical as in Figure 2, and the tie-lines are not straight.

Because phase separation can only take place if $\chi > \chi_c = 4$, it follows from (11) that for any given values of ξ_a and ξ_b there is a critical value of the sticker activity, λ_c, such that phase separation takes place only if $\lambda \geq \lambda_c$. (In Figure 2 λ_c is the lowest point on the coexistence curve, at $\rho = 0.5$). Explicitly

$$\lambda_c = \frac{c - 1}{\xi_b - c\xi_a} \quad (16)$$

where $c = \exp(4/z\nu_b)$. For $\epsilon_b = 2\epsilon_a = 10$ and $z = 12$, $\nu_b = 4$, as in Figure 2, we find that $\lambda_c \approx (c - 1)/\xi_b \approx 4/z\nu_b\xi_b$ is very small, on the order of 10^{-5}. Other reasonable choices of z and ν_a would yield similar estimates. For $\lambda \ll 1$ we have $\lambda \approx \theta_f \ll 1$, indicating that the concentration of free stickers in a phase-separated system is generally very small. Of course, θ_b, the (surface) concentration of binding stickers, is much higher, ensuring the formation of a condensed phase of vesicles. Note also that, at a given temperature, an upper bound on the value of χ is set in the (hypothetical) limit of high concentration of free stickers, ($\lambda \to \infty$). In this limit $\chi \to z\nu_b \ln(\xi_b/\xi_a) = z\nu_b(\epsilon_b - \epsilon_a)$, indicating that $\nu_b(\epsilon_b - \epsilon_a) = \omega_{\text{eff}}$ is the effective pair potential between two vesicles. Indeed, in the limit of high λ all the adsorbing and binding sites on the surface of the vesicles are occupied ($\theta_a, \theta_b \to 1$), implying that $\nu_b(\epsilon_b - \epsilon_a)$ is the energy change associated with bringing two isolated vesicles (already "covered" by stickers) into close, binding, contact. In general, as noted above, condensation already takes place at very low concentrations of stickers.

III. Examples and Analysis

In the two-phase region a dilute phase of vesicles of density ρ_d coexists with a condensed phase of density $\rho_c = 1 - \rho_d$.

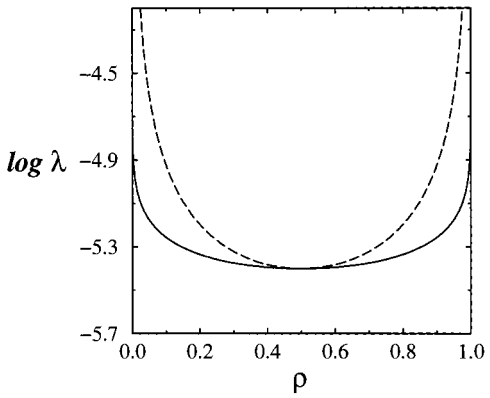

Figure 2. Coexistence (solid) and spinodal (dashed) curves in the ρ − log λ plane, where ρ denotes the volume fraction of vesicles and λ the activity of the stickers. These curves correspond to a system with $z = 12$, $\nu_b = 4$, and $\epsilon_b = 2\epsilon_a = 10$.

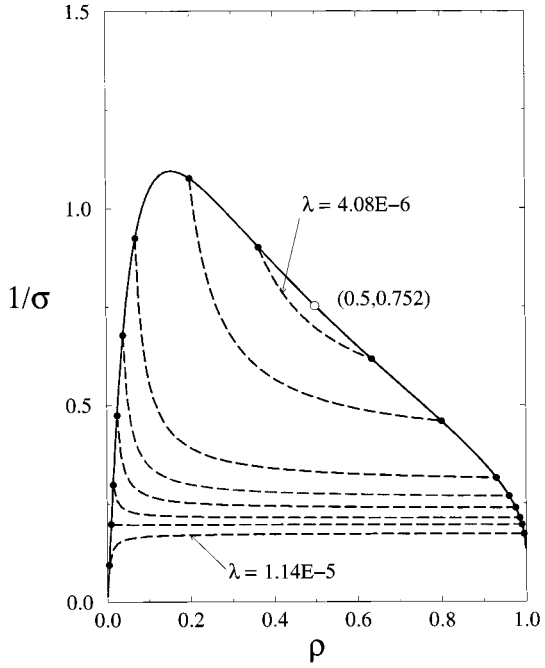

Figure 3. Coexistence (solid) curve, separating between the one- and two-phase regions in the $\rho-1/\sigma$ plane, for a system with $z = 12$, $\nu_b = 4$, $\nu_a = 100$, $\nu_f = 700$, and $\epsilon_b = 2\epsilon_a = 10$. The open circle marks the critical point. The dashed tie-lines correspond to different values of sticker activity λ: from top to bottom, $\lambda/10^{-6}$= 4.08, 4.62, 6.11, 7.08, 7.98, 9.01, 9.88, 11.4.

The chemical potential of the stickers in the two phases are equal, but not their concentrations $\phi = n/M = \sigma\rho$; as before $\sigma = n/N$ denotes the number of stickers per vesicle. For every value of the stickers' activity, λ ($\lambda > \lambda_c$), the values of σ_d and σ_c can be determined using $\sigma_i = \sum_\alpha m_{i,\alpha}(\lambda, \rho_i)\theta_\alpha(\lambda)/M\rho_i$, ($i = d, c$). The $1/\sigma$ vs ρ phase diagrams obtained in this way are shown for two representative cases in Figures 3 and 4. The solid curves in these figures separate between the one- and two-phase regions. The dashed tie-lines connect between the coexistence points, ρ_d, σ_d and ρ_c, σ_c (each pair corresponds to the same values of λ, μ_v, and P). The $\sigma(\rho)$ tie-lines in the two-phase region are calculated using the conservation conditions ("lever rules"), $\rho = \gamma_d\rho_d + \gamma_c\rho_c$ and $\sigma\rho = \gamma_d\sigma_d\rho_d + \gamma_c\sigma_c\rho_c$, where $\gamma_i = M_i/M$ is the volume fraction of the ith phase ($i = d, c$). These two equations yield $\sigma = (\sigma_c - \sigma_d)/\rho + (\rho_c\sigma_c - \rho_d\sigma_d)/(\rho_c - \rho_d)$.

The phase diagram in Figure 3 corresponds to the following choice of model parameters: $z = 12$, $\nu_f = 700$, $\nu_a = 50$, $\nu_b =$

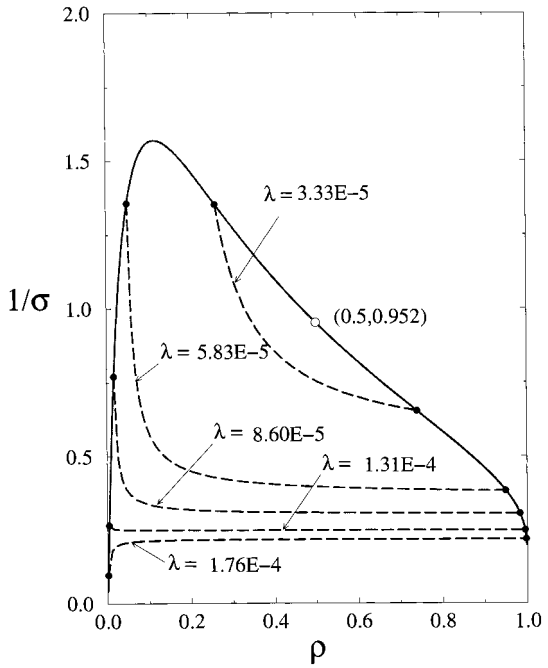

Figure 4. Coexistence (solid) curve, separating between the one-phase and two-phase regions in the $\rho-1/\sigma$ plane, for a system with $z = 4$, $\nu_b = 2$, $\nu_a = 15$, $\nu_f = 50$, and $\epsilon_b = 2\epsilon_a = 10$. The open circle marks the critical point.

4, and $\epsilon_b = 2\epsilon_a = 10$. The results in Figure 4 correspond to $z = 4$, $\nu_f = 50$, $\nu_a = 15$, $\nu_b = 2$, and $\epsilon_b = 2\epsilon_a = 10$. The first set of parameters corresponds, albeit very crudely, to a 3D system of vesicles (of diameter $d \approx 100$ nm) and biotin−avidin−biotin cross-bridges (of cross-sectional area and volume on the order of 30 nm^2 and 10 nm^3, respectively). The values used for ϵ_a and ϵ_b are considerably smaller than those estimated, on the basis of force measurements, for the energies associated with pulling out the chains of the biotinated lipids from their host membrane.[8−13] It should be noted, however, that these measurements provide estimates for the pull-out energy of a stretched lipid chain. On the other hand, once the complex is free in solution (as we assume for our stickers), the hydrophobic lipid tails are mostly likely collapsed, thus reducing the unfavorable exposure of the hydrocarbon chains to water, implying a lower value of ϵ_a as compared to that obtained by force measurements. At any rate, it should be emphasized that our very approximate model calculations are not intended to simulate any specific experimental system but, rather, to provide a qualitative explanation for some of the phenomena observed. In the same spirit, the "molecular" parameters used to obtained the results in Figure 3 correspond to a hypothetical 2D model system. The same parameters were also used in the MC simulations described later in this section.

Returning to Figures 3 and 4 we note that as λ exceeds λ_c and phase separation begins to take place, the average number of stickers per vesicle in the condensed phase is larger than in the dilute phase; $\sigma_c > \sigma_d$. Upon further increasing λ the difference $\Delta\sigma = \sigma_c - \sigma_d$ continues to increase, reaching a maximum, beyond which it decreases monotonically with λ, eventually becoming negative. The crossover from positive to negative $\Delta\sigma$ occurs "deep" in the coexistence region (i.e., when $\rho_d = 1 - \rho_c \ll 1$), where σ_d increases much faster than σ_c. A qualitative explanation of this behavior can be given as follows.

Since for a given λ the θ_α's in both phases are equal, the difference between the $\sigma_{i,\alpha} = \sum_\alpha m_{i,\alpha}(\rho_i)\theta_i/M\rho_i$ reflects the variations of the $m_{i,\alpha}/\rho_i$ with $\rho_i = \rho_i(\lambda)$ ($i = c, d$). For all relevant values of λ (those shown in Figures 3 and 4), $\theta_b \gg \theta_a \gg \theta_f$. Now, an increase in $\lambda - \lambda_c$ implies an increase in $\rho_c - \rho_d$, and hence fast increase of $m_{b,c}$ and fast decrease of $m_{b,d}$. Since the b-stickers provide the main contribution to σ (through m_b) we find that, initially, σ_c increases whereas σ_d decreases. As λ increases further, $\rho_c \rightarrow 1$ whereas $\rho_d \rightarrow 0$, implying that $m_{b,c}$ approaches a finite saturation value ($m_{b,c} \rightarrow z\nu_b/2$), whereas $m_{f,d}/\rho_d$ increases without bound. This explains the rapid increase in σ_d as compared to σ_c at high values of λ (equivalently, ρ_c). Note, however, that for most values of ρ within the two-phase region the majority of stickers are present (as cross-bridges) in the condensed phase. The adsorbed (a) stickers play a secondary role in this interplay as their coverage (θ_a) is the same in both phases.

A conclusion of experimental relevance that can be derived from the calculations shown in Figures 3 and 4 involves the phase behavior of the mixture upon varying the average number of stickers per vesicle (σ) at constant, low, concentration of vesicles, say, $\rho \approx 0.01$, as was done in ref 17. We note that at this, low ρ, region of the phase diagram the phase boundary ($\sigma(\rho)$) increases rapidly with ρ. In other words, σ_d is a very sensitive function of ρ_d; (on the other hand σ_c and ρ_c vary quite slowly). This implies that, at constant (small) ρ, vesicle condensation will only take place if σ exceeds a ceratin minimal value (σ_d); resulting in phase separation between a very dilute and a highly condensed phase of vesicles. Indeed, in the experiments reported in ref 17 it was found that for $\rho \approx 0.01$ no transition takes place when $\sigma = 5$ whereas when $\sigma = 10$ macroscopic aggregates of vesicles appeared in solution, indicating $5 < \sigma_d < 10$.

Finally, in Figure 5 we show four representative snapshots of MC simulations performed on a 2D square lattice, using the same molecular parameters as those in the mean-field calculations of Figure 4 ($\nu_f = 50$, $\nu_a = 15$, $\nu_b = 2$, $z = 4$, $\epsilon_b = 2$, $\epsilon_a = 10$). Of course, we do not expect to find quantitative agreement between the mean-field predictions and the simulations. (It is well-known, for example, that the mean-field value of the critical interaction parameter $\chi_c = 4$ of an interacting 2D lattice is about 1.75 times smaller than the exact value.[18])

The simulations were performed in the same (N, λ, M, T) statistical ensemble as the mean-field calculations. That is, N particles (vesicles) were allowed to move on a $M = 100 \times 100$ square 2D lattice, with periodic boundary conditions. More explicitly, choosing a given sticker activity, λ, random MC moves were attempted and accepted or rejected according to the usual Metropolis criterion, using $\Delta E = F_s(\{C'\}) - F_s(\{C\})$ as the "energy difference" associated with the attempted move; $F_s(\{C'\})$ and $F_s(\{C\})$ denote the free energies corresponding, respectively, to the final and initial configurations of the vesicles, cf. (1). Note that the stickers are not explicitly included in the simulation. Their distribution among the various vesicles, for any configuration $\{C\}$, was calculated using the chemical equilibrium conditions (4). More explicitly, in each MC step, the interaction energy between two neighboring vesicles was calculated as $\nu_b\theta_b\epsilon_b$, with θ_b calculated using (3) and (4). Similarly, the energy of an isolated vesicle is given by $z\nu_a\theta_a\epsilon_a$, etc. In other words, in these simulations the distribution of stickers is equilibrated at each MC step. Physically, this assumption is valid when the lateral diffusion of the stickers over the vesicle surfaces and in and out of the bulk is instantaneous (on the time scale of vesicle diffusion), regardless of the barrier heights associated with such transitions. Thus, these simulations are only valid for a fully equilibrated system.

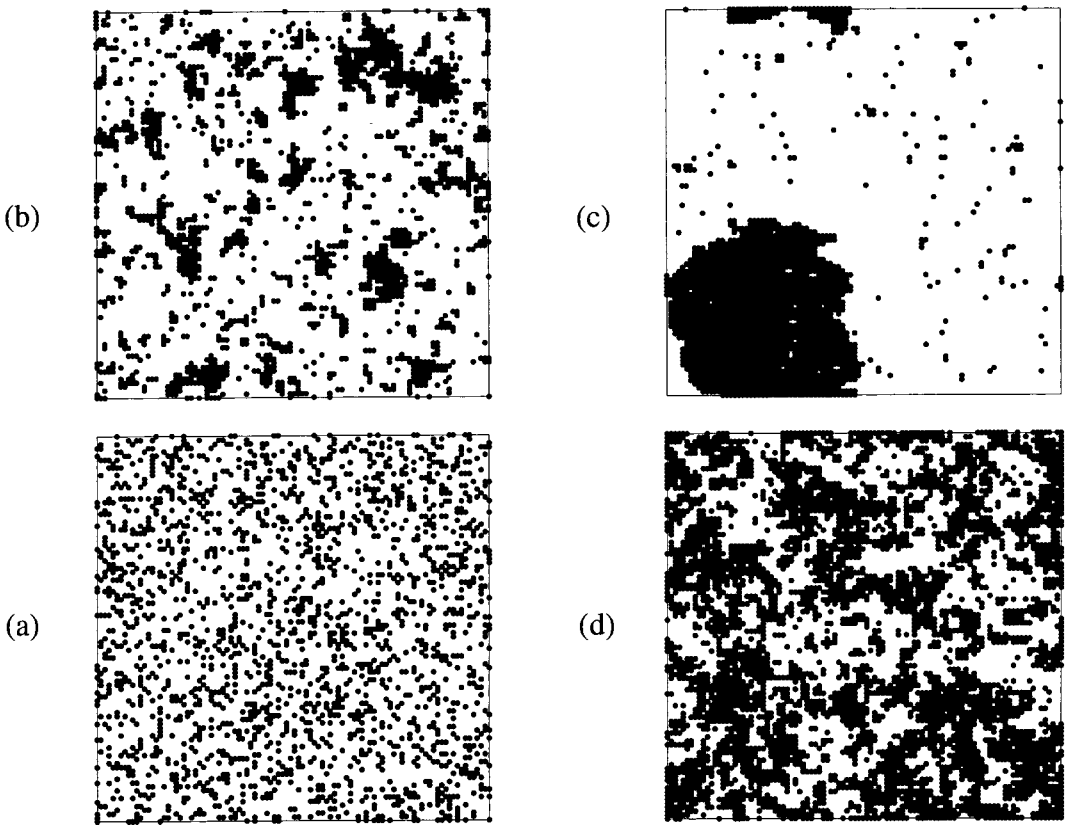

Figure 5. Four representative snapshots from the Monte Carlo simulations described in the text. Snapshots a, b, and c correspond to the same value of the vesicle density, $\rho = 0.2$, with $\sigma = 0.16$, 1.8, and 3.3, respectively; (a) and (b) correspond to the one-phase region whereas (c) is well inside the two-phase region. In snapshot d $\rho = 0.5$, $\sigma = 2.0$, corresonding to near-critical conditions.

Three of the snapshots shown in Figure 5 (a, b, and c) correspond to the same vesicle density, $\rho = 0.2$, but different values of the sticker activity λ and hence different values of σ. The values of σ were calculated using the appropriate λ and the average values of N_{vv},N_{v0},N_{00} as obtained from the simulations. In Figure 5a, the sticker concentration is too low and the system is uniform. As σ increases large clusters appear, but the system is still one-phasic, very near the coexistence curve; see Figure 5b. In Figure 5c the system is already well within the two phase region, showing very clearly the coexistence of dilute and condensed vesicle phases. Figure 5d shows a typical snapshot in the vicinity of the critical point, displaying the familiar structures of near-critical clusters.

IV. Summary

The statistical thermodynamic description of a solution containing two types of solutes of different sizes, which are governed by specific adsorption and binding interactions, such as the vesicle−sticker mixture considered in this work, is rather complicated. Our mean-field approach to this problem, whereby the occupations of sticker adsorption and binding sites on vesicle surfaces are replaced by their statistical averages, greatly simplifies this description. This approximate treatment becomes even simpler upon transforming from the two-component canonical ensemble (N, n, M, T) to the mixed, canonical-grand ensemble (N, λ, M, T), where the various sticker populations are determined by the two variables, λ and $\rho = N/M$. In particular, λ, which controls the occupation probabilities of adsorbed and binding sites, also governs the effective interaction potential between the vesicles. Thus, it is not surprising that the phase behavior predicted by Figure 2 and illustrated by MC simulations in Figure 5 appears identical to that of an ordinary interacting lattice gas. These results become more relevant upon transforming to experimentally controllabe parameters, such as the vesicle and sticker concentrations: ρ and σ.

In addition to the inherent limitations associated with any mean-field treatment and lattice model, we have made a number of assumptions in order to simplify the underlying physical picture. For example, we have assumed that all adsorption sites are equivalent and that the adhesion energy between two vesicles is simply proportional to the number of binding contacts, thus ignoring nonadditive effects associated with sticker−sticker interactions and membrane elasticity. Notwithstanding these reservations, the simple model described in this work provides a convenient, albeit mainly qualitative, scheme for analyzing the equilibrium phase behavior of a system of particles governed by cross-bridge mediated adhesion. Of course, this scheme is not appropriate for describing the kinetic behavior of such systems nor the appearance of metastable structures. Yet, any metastable kinetic behavior should at least be contrasted with the corresponding equilibrium thermodynamics of the system in question.[19] This has been our goal in this paper.

Acknowledgment. We thank Joe Zasadzinski and Scott Walker for several helpful discussions and for information concerning their unpublished experimental results. This work was supported by the U.S.−Israel Binational Science Foundation and by the Israel Science Foundation. The Fritz Haber research center is supported by the Minerva Foundation, Munich, Germany.

References and Notes

(1) See, e.g.: Livna, O.; Bayer, A.; Wilchek, M.; Sussmann, J. L. *Proc. Natl. Acad. Sci. U.S.A.* **1993**, *90*, 5076 and references therein.

(2) Noppl-Simon, D. A.; Needham, D. *Biophys. J.* **1996**, *70*, 1391.
(3) Bell, G. I. *Science* **1978**, *618* and refernces therein.
(4) Dembo, M.; Torney, D. C.; Saxman, K.; Hammer, D. *Proc. R. Soc. London* **1988**, *B234*, 55.
(5) Lynch, N. J.; Kilpatrick, P. K.; Carbonell, R. G. *Biotechnol. Bioeng.* **1996**, *50*, 151.
(6) von Schulthess, G. K.; Benedek, G. B.; De Blois, R. W. *Macromolecules* **1983**, *16*, 434.
(7) Evans, E. A. *Biophys. J.* **1985**, *48*, 175.
(8) Leckband, D. E.; Schmitt, F. J.; Israelachvili, J. N.; Knoll, W. *Biochemistry* **1994**, *33*, 4611.
(9) Leckband, D. E.; Muller, W.; Schmitt, F. J.; Ringsdorf, H. *Biophys. J.* **1995**, *69*, 1162.
(10) Florin, E. L.; Moy, V. T.; Gaub, H. E. *Science* **1994**, *264*, 415.
(11) Moy, V. T.; Florin, E. L.; Gaub, H. E. *Science* **1994**, *266*, 257.
(12) Evans, E. In *Structure and Dynamics of Membranes*; Lipowsky, R., Sackmann, E., Eds.; North-Holland: Amsterdam, 1995; Chapter 15.
(13) Ciruvolu, S.; Walker, S.; Israelachvili, J. N.; Schmitt F. J.; Leckband D.; Zasadzinski J. A. *Science* **1994**, *264*, 1753.
(14) Lee, G. U.; Kidwell, D..; Richard J. C.; *Langmuir* **1994**, *10*, 354.
(15) Chilkoti, A.; Boland, T.; Ratner B. D.; Stayton, P. S. *Biophys J.* **1995**, *69*, 2125.
(16) Grubmüller, H.; Heymann B.; Tavan P. *Science* **1996**, 271, 997.
(17) Walker, S. Ph.D. Thesis, University of California Santa Barbara, 1997.
(18) See, e.g.: Hill, T. L. *An Introduction to Statistical Thermodynamics*; Addison-Wesley: Reading, MA, 1960.
(19) Levine, R. D.; Bernstein, R. B. *Molecular Reaction Dynamics and Reactivity*, 2nd ed.; Oxford University Press: Oxford, 1989.